

Study The Proton Momentum Distribution of The $^{51}\text{V}(\gamma,p)^{50}\text{Ti}$ Reaction at Energy of 59.2 Mev

Dr. Alaa .B. Kadhim*, Raafat. A. Muslim**, Dr. Khaled. H. Mahdi**
& Fouad. N. Hassan*

Received on: 30/8/2010

Accepted on: 7/4/2011

Abstract

The technique developed by Findlay and Owens for the extraction of a consistently effective momentum distribution from the $^{51}\text{V}(\gamma,p)^{50}\text{Ti}$ reaction data is applied to the cross sections obtained for each of the discrete low lying excited states (0.0 , 1.6 , 2.7 , 3.2 , 3.8 , 4.4 and 6.0) MeV ,respectively.The momentum density and momentum mismatch have been calculated using the method of Findlay and Owens for each excited state. This program has been written for this purpose using Fortran-77 language.The momentum scaled distribution would illustrate that the simple Direct Knockout Model (DKM) behavior observed in the (γ,p) reaction could be regarded as evidence for the importance of the DKM process in the (γ,p) reaction. Clearly the application of the procedure given by Findlay and Owens leads to a more consistent momentum distribution.

دراسة توزيع وخم البروتونات للتفاعل $^{51}\text{V}(\gamma,p)^{50}\text{Ti}$ عند الطاقة 59.2 MeV

الخلاصة

استخدمت تقنية فندلي واونز المتطورة لاستخراج توزيع الزخم الفعال من بيانات التفاعل $^{51}\text{V}(\gamma,p)^{50}\text{Ti}$ للمقاطع العرضية المستحصلة لكل مستويات الطاقة المتهيجة الواطنة المنفصلة MeV (0.0 , 1.6 , 2.7 , 3.2 , 3.8 , 4.4 , 6.0) على التوالي . كثافة الزخم والزخم المفقود تم حسابهما باستعمال تقنية فندلي واونز لكل حالة متهيجة. كتب برنامج بلغة فورتران- 77 اعد لهذا الغرض . توزيع الزخم المدرج يوضح سلوك نموذج هروب الجسيمة الواحدة البسيط (DKM) الملاحظ في تفاعل $^{51}\text{V}(\gamma,p)^{50}\text{Ti}$ حيث يمكن ان يعتبر كدليل لاهمية عملية (DKM) في التفاعل (γ,p) ومن الواضح ان تطبيق هذه الطريقة المعطاة من قبل فندلي واونز تؤدي الى انسجام اكبر لتوزيعات الزخم المحسوب .

Introduction

Photons with energies less than 30 MeV are known to interact coherently with the whole nucleus as giant dipole resonance. Photons with energy greater than 30 MeV and less than 100 MeV have significantly shorter wavelength. At this range of energy the photon interact with just a single nucleon or a small group of nucleons within the

nucleus. One possible result of the absorption of such a photon is that a single nucleon will be ejected with an energy equal to or close to the kinematic end for that reaction. The other nucleons are essentially spectators in the process [1-4]. If we consider the reaction $^{51}\text{V}(\gamma,p)^{50}\text{Ti}$ in which the ^{50}Ti is left in its ground state or low lying excited state then

*College of Science, University of Baghdad/Baghdad

**College of Education Ibn-Hatham, University of Baghdad/Baghdad

photons with energy $E_\gamma \approx 60$ MeV would produce protons leaving the nucleus with a momenta in the range of 330 to 390 MeV/c, depending on the emission angle. However the incoming photons have a momentum of only 60 MeV/c thus creating a momentum mismatch which must be supplied by the residual nucleus (equal to its recoil momentum in lab system). If the (γ, p) reaction is considered as the photon strikes a single nucleon in a specific subshell and is ejected it from the nucleus. Then the other nucleons are unaffected. Hence the cross sections for such a reaction will depend on the nucleon momentum distribution inside the nucleus and the form of final state potential. This nucleon momentum distribution could be calculated from a nucleon model, such as the Independent Particle Shell Model (IPSM), and with a proper treatment of the final state interaction [5,6].

Calculations

The calculations used on the (γ, p) data are based upon the method by Findlay and Owens [7,8]. They have tried to eliminate the effects of distortion in the final state of the (γ, p) reaction, in order to obtain the undistorted momentum distribution in the initial nucleus.

In the Plane Wave Impulse Approximation (PWIA) the (γ, p) reaction cross sections are directly proportional to the probability of finding a proton of the appropriate momentum in the initial state. Findlay and Owens have provided an approximation treatment of the distortion with regards to outgoing proton wave potential of the residual nucleus, while keeping the direct relationship between the cross

sections and the momentum distribution unchanged.

In this method the real and imaginary parts of the optical potential are treated separately. The main effect of the real part is to reduce the energy of the proton, without much effecting its direction as it leaves the nucleus. The observed outgoing proton momentum $\hbar k$ is thus related to the internal momentum $\hbar k_i$ just after the photon is absorbed by [7,8]:

Where A is the mass number of ^{51}V , and m_p is the mass of proton.

The real part of the optical potential $U(E)$ is given by [7,8]:

$$(\hbar k_i)^2 - (\hbar k)^2 - 2m_p \left(1 - \frac{1}{A}\right) [U(E)] \dots\dots\dots (1)$$

Where V_o is the depth of the well $U(E) = -V_o [1 - 1.015 \tanh(0.005E)] \dots\dots (2)$ and is equal 28 MeV and calculated by [9]:

$$V_o = E_f + S_p \dots\dots (3)$$

Where E_f is Fermi energy as given by [9]:

$$E_f = \frac{\pi^2 \hbar^2}{2m_p} \left(\frac{3n}{\pi}\right)^{2/3} \dots\dots\dots (4)$$

Where n is the number of nucleons per unit volume.

And S_p is the separation energy of the proton and given by [9]:

$$S_p = [M(A-1, Z-1) + m_p - M(A, Z)]c^2 \dots\dots (5)$$

Where $M(A-1, Z-1)$ is the mass of the residual nucleus, and $M(A, Z)$ is the mass of the original nucleus.

In this approximation, the cross section for the (γ, p) reaction in the center of mass system for the photoproton ejected from an active shell "momentum density of the proton" is given by[7,8]:

$$\psi(\vec{q}) = \frac{\frac{d\sigma}{d\Omega}}{\left\{ 2\pi \frac{A-1}{A} \frac{e^2}{m_p c^2} \frac{\hbar^2 k_p^2}{2m_p} \sin^2 \theta_p \left(1 - \frac{\partial v}{\partial E} \right) \eta(E) v_p \right\}} \dots (6)$$

All quantities are defined in the center of mass system. Where v_p is the proton occupation number of the active subshell, $\left(1 - \frac{\partial v}{\partial E} \right)$ is the pare factor [10]. The effect of the imaginary component approximated as an energy – independent absorption factor η , where its value was estimated as $\eta = 0.4$, and q is the initial momentum of the proton in the bound state, and is given by[7,8]:

$$\hbar \vec{q} = \hbar \vec{k}_p - \left(1 - \frac{1}{A} \right) \hbar \vec{k}_\gamma \dots (7)$$

Where θ_p is the angle of emission of the photoproton, and $\hbar \vec{k}_\gamma$ is the incoming photon momentum.

Now, it is possible to calculate $\psi(\vec{q})$ in the active subshell from each differential cross section $\frac{d\sigma}{d\Omega}$ data point corresponding to a given proton emission angle and photon energy.

Calculations have been performed by writing the program in FORTRAN – 77 language and the flowchart is of the program as shown in figure (1). This program explains the steps of calculations:

Results and Discussion

We have performed calculations for the $^{51}\text{V}(\gamma, p)^{50}\text{Ti}$ reaction data obtained [11] over a wide range of angles from 61° to 110° . The incident photon energy was about 60 MeV and low lying excited states were as follow (0.0 , 1.6 , 2.7 , 3.2 , 3.8 , 4.4 and 6.0) MeV. They are compared to existing data in order to assess the extent to how the Direct Knockout Mechanism(DKM) contributes to the observed cross sections.

Figures (2,4,6,8,10,12,14) shows the differential cross sections as a function of proton angles at energy about 60 MeV for different excited states. Figures (3,5,7,9,11,13,15) shows the momentum density as a function of the missing momentum for all the excited state shown in the following figures.

In conclusion the results indicate that the (DKM) mechanism is the main contributor to the cross sections for low missing momentum. Should there be any deviations found in large momenta then we can deduce that the Quasi Deuteron Model (QDM) mechanism has contributed. Furthermore, It was also confirmed possible to extract a unique momentum distribution up to momenta of 390 MeV/c from data on the $^{51}\text{V}(\gamma, p)^{50}\text{Ti}$ reaction. In all figures, a good agreement in behavior and shape is ascertained.

Reference

[1] **J.L.Matthews, D.J.S.Findlay, S. N.Gardiner, R.O.Owens.** High energy photoprotons from light nuclei // *Nucl. Phys. A.*1976, v. 267, p. 51-76.
 [2]- **M.Gari and H. Hebach,** physics reports(Review Section of Physics Letters)72. No.1(1981) 1-55.
 [3]- **M.R.Sene, I.Anthony, D.Bean-**

- ford, A.G.Shotter, R.O.Owens,
Nuclear Physics A442(1985) 215-
233.
- [4]- C.Segebade,H.P.Weise and
G.J.Lutz,PhotonActivation
Analysis (1987).
- [5]- **Mattias Hldenhov**, Ph.D.thesis,
University of Lund, Sweden (2005).
- [6]- **P. Lilja**, Ph.D. thesis, University
of Lund, Sweden (2004).
- [7]- **D.J.S.Findlay and R.O.Owens**,
Nucl.Phys.A292 (1977) 53.
- [8]- **D.J.S. Findlay and R.O.Owens**,
Phys .Rev.Lett 37 (1976) 674.
- [9]- **M.Hibeeb**, 2008, The nuclear
physics fundamentals, 1, daralfiker.
- [10]- **F.G.Perey**, in
Direct Interaction and Nuclear
Reaction Mechanism, edited by
E.Clemental and C.Villi,New
York,1963, P. 125; T.de
Forest,Nucl. A163, 237(1971).
- [11]- D.G.Ireland,D.Branfoed,
T.Davinson,N.J.Davis,E.W.
Macdonald,P.J.Sellin,A.C.Shotter,P.T
erzoudi,P.J.Woods,J.O.Adler,B.E.An
derson,L.Isaksson,D.Nilsson,H.Ruijter,
A.Sandell,B.Schroder,J,NP/A,554,1
73,1993.

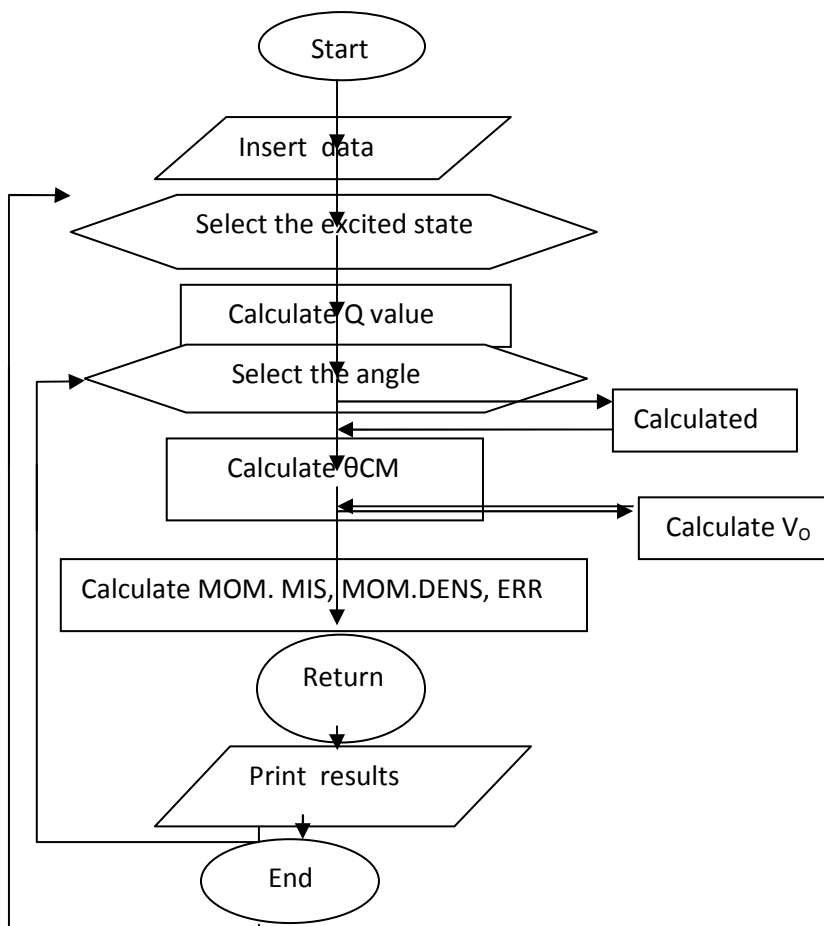


Figure 1 flowchart of program

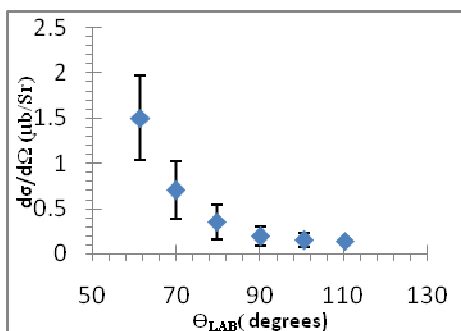


Figure2 The angular distribution for $^{51}\text{V}(\text{G}, \text{P})^{50}\text{Ti}$ reaction in 0.0 MeV excited states

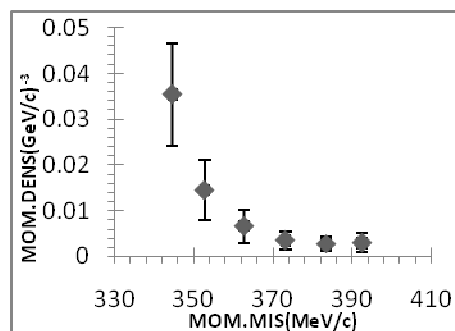


Figure 3 The momentum distribution for $^{51}\text{V}(\text{G}, \text{P})^{50}\text{Ti}$ reaction in 0.0 MeV excited states

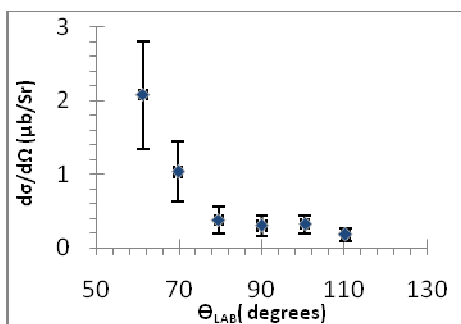


Figure 4 The angular distribution for $^{51}\text{V}(\text{G}, \text{P})^{50}\text{Ti}$ reaction in 1.6 MeV excited states

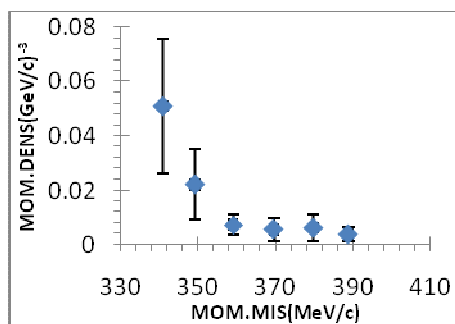


Figure 5 The momentum distribution for $^{51}\text{V}(\text{G}, \text{P})^{50}\text{Ti}$ reaction in 1.6 MeV excited states

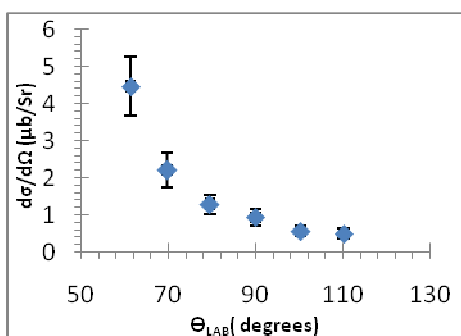


Figure 6 The angular distribution for $^{51}\text{V}(\text{G}, \text{P})^{50}\text{Ti}$ reaction in 2.7 MeV excited states

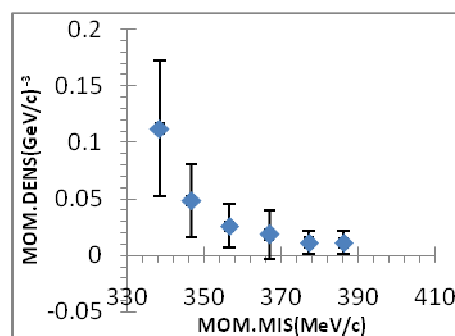


Figure7 The momentum distribution for $^{51}\text{V}(\text{G}, \text{P})^{50}\text{Ti}$ reaction in 2.7 MeV excited stat

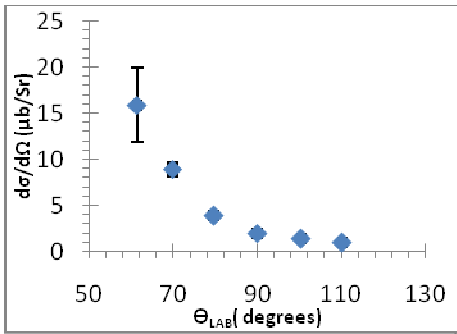


Figure 8 The angular distribution for $^{51}\text{V}(\text{G},\text{P})^{50}\text{Ti}$ reaction in 3.2 Me V excited states

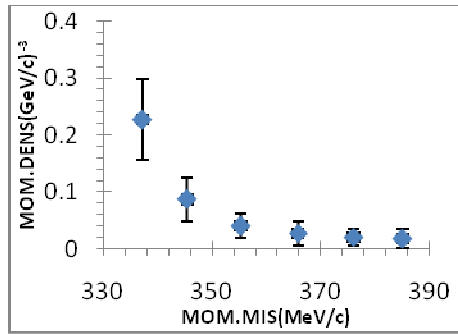


Figure 9 The momentum distribution for $^{51}\text{V}(\text{G},\text{P})^{50}\text{Ti}$ reaction in 3.2 MeV excited states

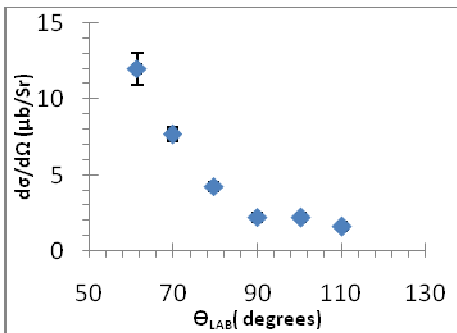


Figure 10 The angular distribution for $^{51}\text{V}(\text{G},\text{P})^{50}\text{Ti}$ reaction in 3.8 Me V excited states

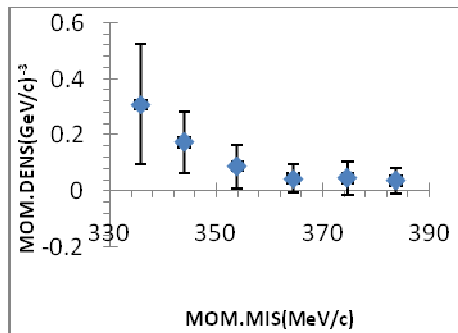


Figure 11 The momentum distribution for $^{51}\text{V}(\text{G},\text{P})^{50}\text{Ti}$ reaction in 3.8 MeV excited states

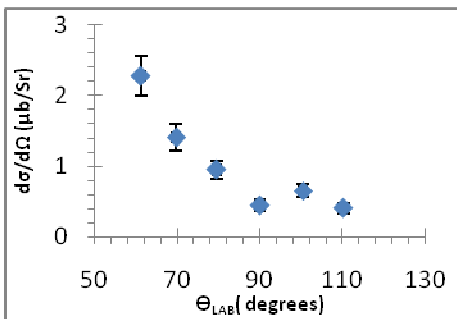


Figure 12 The angular distribution for $^{51}\text{V}(\text{G},\text{P})^{50}\text{Ti}$ reaction in 4.4 Me V excited states

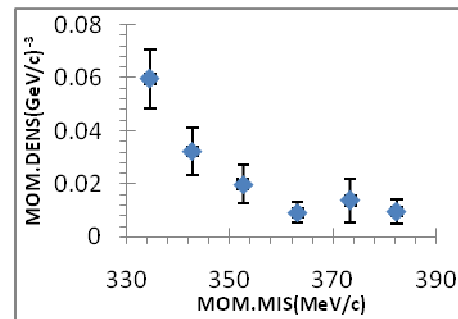


Figure 13 The momentum distribution for reaction in 4.4 MeV excited states

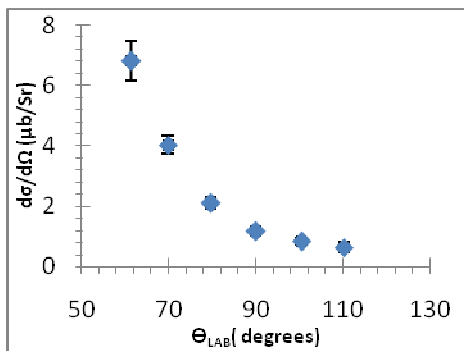


Figure14 The angular distribution for $^{51}\text{V}(\text{G}, \text{P})^{50}\text{Ti}$ reaction in 6.0 Me V excited states

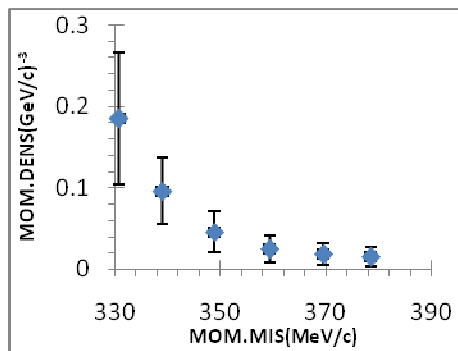


Figure15 The momentum distribution for $^{51}\text{V}(\text{G}, \text{P})^{50}\text{Ti}$ reaction in 6.0 MeV excited states